

Dual-beam delay-encoded all fiber Doppler optical coherence tomography for *in vivo* measurement of retinal blood flow

Mingming Wan (万明明)^{1,†}, Shanshan Liang (梁姗姗)^{2**,†}, Xinyu Li (李新宇)³, Zhengyu Duan (段铮昱)⁴, Jiebin Zou (邹杰斌)¹, Jun Chen (陈军)^{1,5}, Jin Yuan (袁进)⁶, and Jun Zhang (张军)^{7*}

¹School of Electronics and Information Technology, Sun Yat-sen University, Guangzhou 510006, China

²National Innovation Center for Advanced Medical Devices, Shenzhen 518131, China

³GBA Branch of Aerospace Information Research Institute, Chinese Academy of Sciences, Guangzhou 510530, China

⁴School of Biomedical Engineering, Sun Yat-sen University, Guangzhou 510006, China

⁵State Key Laboratory of Optoelectronic Materials and Technologies, School of Electronics and Information Technology, Sun Yat-sen University, Guangzhou 510275, China

⁶State Key Laboratory of Ophthalmology, Zhongshan Ophthalmic Center, Sun Yat-sen University, Guangzhou 510060, China

⁷School of Artificial Intelligence, Guilin University of Electronic Technology, Guilin 541004, China

*Corresponding author: junzhang8819@gmail.com

**Corresponding author: ss.liang@nmed.org.cn

Received September 2, 2021 | Accepted October 14, 2021 | Posted Online November 8, 2021

In this paper, we propose and demonstrate a dual-beam delay-encoded Doppler spectral domain optical coherence tomography (OCT) system for *in vivo* measurement of absolute retinal blood velocity and flow with arbitrary orientation. The incident beam is split by a beam displacer into two probe beams of the single-spectrometer spectral domain OCT system with orthogonal polarization states and an optical path length delay. We validate our approach with a phantom and *in vivo* experiments of human retinal blood flow, respectively.

Keywords: optical coherence tomography; ocular perfusion; optic nerve head; ophthalmology.

DOI: [10.3788/COL202220.011701](https://doi.org/10.3788/COL202220.011701)

1. Introduction

Abnormalities in eye perfusion have been linked to a number of sight-threatening diseases including glaucoma, retinal vein occlusions, diabetic retinopathy, age-related macular degeneration^[1-3], etc. Optical coherence tomography (OCT)^[4,5], a technology offering high-resolution cross-sectional imaging of microstructures in biological tissues, has been widely used in clinical medicine^[6-9]. In addition to morphological images, the functional OCT technology, such as OCT angiography^[10,11] and Doppler OCT (DOCT)^[12-15], has been proposed to calculate the retinal vessel information.

The disadvantage of conventional single-beam DOCT system is that flow velocity measurement depends on the Doppler angle between the incident beam and blood vessel orientation. Therefore, some researchers suggested using dual-beam detection systems to overcome this problem^[16]. In 2000, Dave *et al.* first, to the best of our knowledge, demonstrated a dual-channel DOCT system based on a Wollaston prism for absolute velocity measurement in highly scattering media^[17]. In 2014,

Werkmister *et al.* presented a dual-beam spectral domain DOCT system using a beam displacer to split a beam of light into two detection beams with different polarization states^[18,19]. However, this free space approach requires two separate reference arms and two spectrometers for detection, which increases the cost and complexity of the system. Pedersen *et al.*^[20,21] introduced a glass plate into the OCT beam path to divide it into two probe beams with different group delays and incident angles. However, due to the strong crosstalk between the two probe beams, the achievable depth range is limited. On the other hand, other research groups have also implemented the indirectly bidirectional scanning method through measuring the Doppler tomography at adjacent vessel cross sections within the 3D data volume^[22-25]. For instance, Wang *et al.* adopted only two cross-sectional scans at different positions along the blood vessel to obtain absolute retinal flow velocity. Furthermore, they measured total retinal blood flow (TRBF) by scanning around the optic nerve head (ONH) in two concentric circles^[26,27]. However, the accuracy of blood flow measurement is limited

by the estimation of the vessel center location. Moreover, the demonstrated DOCT systems based on the time division dual-beam to calculate the incident angle are still complex and easily affected by the movement of the eye. Compared with bi-directional approaches, the triple-beam OCT method^[28,29] is independent of the *en face* angle for absolute velocity calculation. However, due to necessary average division of illumination power among the three channels, this triple-beam method suffers from reduced sensitivity. To avoid this division of illumination power, Wartak *et al.*^[30] introduced an active-passive channel approach using path length encoding to achieve triple-channel DOCT. However, the passive channels exhibit more susceptibility to the ocular aberrations than the active channel. In 2018, Wartak *et al.*^[31] introduced an optical switching to achieve time-encoded triple-channel DOCT. Similarly, the time division triple-channel system is also easily affected by the movement of the eye and decreases the imaging speed.

In this paper, we describe a dual-beam delay-encoded all fiber DOCT system (DDD-OCT) using only one spectrometer to measure the TRBF. Compared with Refs. [20,21], a beam displacer splits a beam of detection light into two probe beams in the sample arms that are delay-coded with different optical path lengths using a glass plate, which avoids the crosstalk between two channels. With this technique, only one spectrometer is required. A Dove prism^[32] is used to perform the rotation of the two probe beams. The integrated unit of line scanning laser ophthalmoscopy (LSLO) is used to preview the fundus and guide the scanning track of OCT beams on the retina. The *in vivo* study demonstrates the ability of the DDD-OCT to measure the retinal blood flow.

2. Materials and Methods

Figure 1 shows the setup of the DDD-OCT. The light source is a low coherence superluminescent diode (SLD, Inphenix Inc.) with a central wavelength of 850 nm and an FWHM bandwidth of 50 nm. The lateral resolution is 22 μm , and the coherence

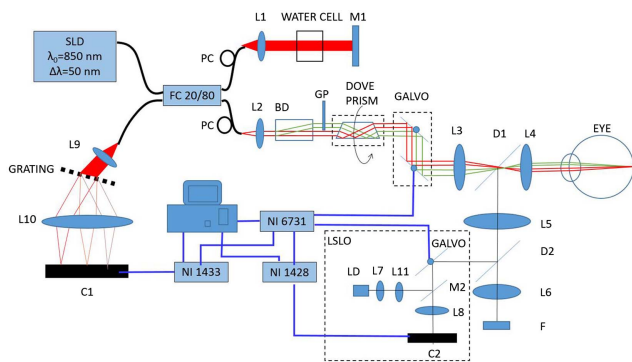


Fig. 1. Schematic of the dual-beam delay-encoded fiber-based DOCT system. L1–L10, lens; L11, cylindrical lens; M1, mirror; M2, strip mirror; D1, D2, dichroic mirror; C1, C2, line scan camera; FC, fiber coupler; PC, polarization controller; F, fixation screen; GP, glass plate; BD, beam displacer; LD, 780 nm laser diode; LSLO, line scanning laser ophthalmoscopy system; SLD, superluminescent diode.

length is 4.64 μm in tissue ($n = 1.37$) for this OCT system. A calcite beam displacer (Fujian Crystock, Inc.) splits the light into two probe beams with a parallel displacement of 2.8 mm. The two probe beams with a diameter of 1.19 mm each are displaced by 1.23 mm on the pupil of the eye. A tiltable glass plate is inserted into one of the probe beams to adjust the optical path length delay (currently 750 μm) between the two probe beams. In the detection arm, the dual-beam OCT signal is detected by only one spectrometer, which is composed of a diffraction grating (Wasatch Photonics, 1200 lines/mm), an achromatic lens (L10, $f = 187$ mm), and a 2048 element line scan CMOS camera C1 (BASLER SPL2048–70 KM). The system is operated at a rate of 50,000 lines/s. The total incident light power of the two probe beams on the cornea is 680 μW , which is well within the maximum permissible exposure level of the American National Standards Institute (ANSI).

The LSLO system is used to provide real-time fundus preview imaging and guide the scanning position of OCT sampling beams, which is composed of a cylindrical lens (L11) that diverges the light beam from a 780 nm laser diode (LD) in a straight line, a strip gold mirror (M2) that isolates the entrance aperture from the exit aperture, and a line scan camera C2 (Atmel AVIIVA SM2 2014). The incident light power of the LSLO on the cornea is measured to be 1 mW, which is below the ANSI safety limit.

As shown in Fig. 2, the incident probe beams P_1 and P_2 are angularly separated by the angle $\Delta\alpha$. The *en face* angle β is defined as the angle between the illumination plane (composed of P_1 and P_2) and the blood flow velocity vector V . For a dual-beam system, calculation of the absolute blood velocity is independent of the Doppler angle (the angle between the incident beam and blood vessel orientation). The absolute blood velocity can be given as^[33]

$$V = \frac{(\phi_2 - \phi_1)\lambda_0}{4\pi n\tau \cdot \cos \beta \cdot \Delta\alpha}, \quad (1)$$

where τ is the time interval between two sequential A-lines, λ_0 is the central wavelength of the SLD, ϕ_1 and ϕ_2 are the phase value of P_1

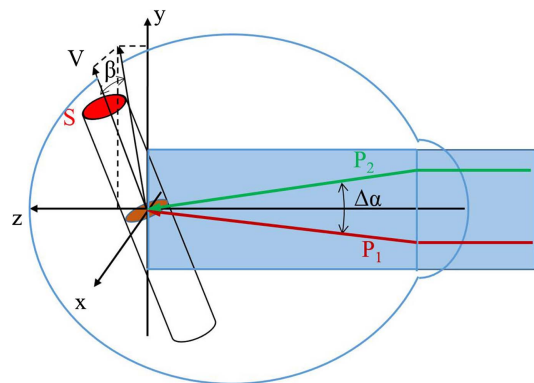


Fig. 2. Illustration of the incident probe beams and the blood flow velocity. V , direction of the blood flow velocity; P_1 and P_2 , two probe beams; $\Delta\alpha$, angle between the two probe beams; β , angle between V and the illumination plane (y - z plane, composed of P_1 and P_2).

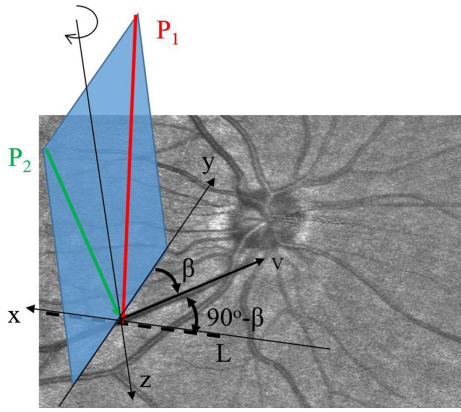


Fig. 3. Illustration of the illumination plane and scanning track. V , direction of the blood flow velocity; L , scanning track of OCT beams on the retina.

and P_2 , respectively, and n is the refractive index of blood. The angle $\Delta\alpha$ relies on the beam separation at the pupil and the eye length (24.2 mm)^[34]. Since the absolute velocity measurement is not accurate when β approaches 90° , then a rotatable Dove prism is used to adjust the orientation of the illumination plane, which can maintain β away from 90° for every probed vessel. In case of a large *en face* angle β , the measured phase difference ($\phi_2 - \phi_1$) is too small to accurately calculate blood flow velocity, especially for slow blood flow velocity. Therefore, as shown in Fig. 3, the scanning track L should be away from the parallel direction of the blood flow V by rotating a calibrated angle to ensure the *en face* angle β is away from 90° .

According to Eq. (1), the blood flow can be calculated as

$$F = \iint_S V dS dt = \iint_{S_{xz}} V \cdot dS_{xz} \cdot \cos \beta dt$$

$$= \iiint_{S_{xz}} \frac{(\phi_2 - \phi_1)\lambda_0}{4\pi n \tau \cdot \Delta\alpha} dx dz dt, \quad (2)$$

where S is the cross-sectional area of the vessel, and $S_{xz} = S / \cos \beta$ (Fig. 2) represents the scanned cross-sectional area of the vessel. Therefore, the absolute blood flow is independent of the angle β ^[35].

3. Results

An *in vitro* experiment is carried out to verify our method. A capillary with an inner diameter of $135 \mu\text{m}$, perfused with chicken blood at a constant flow velocity by a syringe pump, is used as the phantom sample. The capillary is immersed in diluted milk to suppress surface reflection. The calculation accuracy of the Doppler frequency shift depends on the sampling step between adjacent A-scans. In order to determine the optimized sampling step, the phantom flow at various sampling steps is measured to be compared with the set blood flow of $20 \mu\text{L}/\text{min}$. As shown in Fig. 4(a), the accuracy of the measurement can be ensured with a sampling step less than $1.9 \mu\text{m}$. In our experiment, the step spacing is chosen to be $1 \mu\text{m}$.

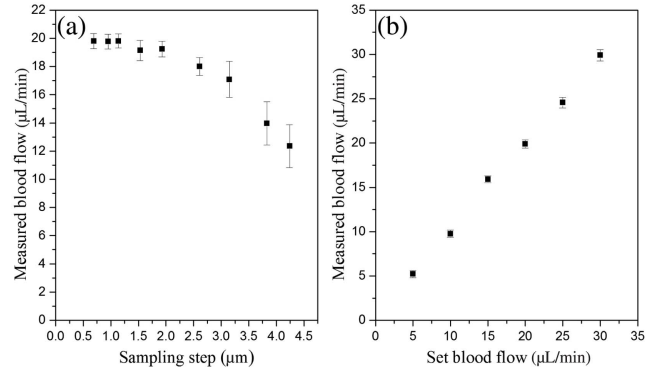


Fig. 4. (a) Measured blood flow at the set blood flow of $20 \mu\text{L}/\text{min}$ as a function of the sampling step. (b) Measured blood flow versus the set blood flow.

The measurement error of the system is within 10% [Fig. 4(b)], showing good accuracy and repeatability.

To verify the system *in vivo* study, the blood flow in the retina of four healthy volunteers is imaged with the DDD-OCT system. This clinical study was approved by the Institutional Review Board of the Zhongshan Ophthalmic Center, Sun Yat-sen University, China and adhered to the tenets of the Declaration of Helsinki. The vessels with diameters above $60 \mu\text{m}$ are taken to calculate the TRBF. Informed consent is obtained from the subject before the experiment.

The probe beams are scanned around the ONH, as shown in Fig. 5(a), to determine the TRBF. The structural and DOCT images of the artery vessel V_1 incident with the probe beams P_1 and P_2 are shown in Figs. 5(b) and 5(c), respectively, without clear crosstalk between two channels. Figure 5(d) illustrates the absolute velocity of the blood flow with a pulsation

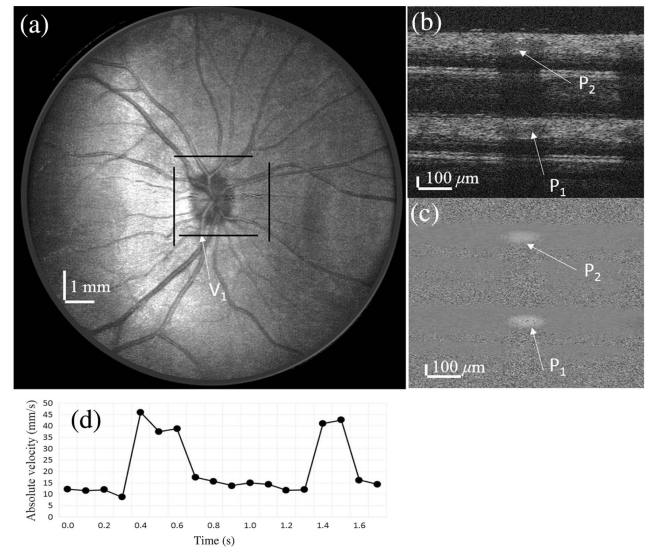


Fig. 5. Retinal blood flow imaging with the DDD-OCT system. (a) LSO fundus view. The black line marks the scanning track. V_1 , an artery vessel. (b) Structural and (c) Doppler OCT images of the vessel V_1 . (d) Absolute velocity of the blood flow in V_1 as a function of time.

rate of 67 beats/min. The average absolute flow of the artery vessel V_1 in a cardiac cycle is calculated to be 12.2 $\mu\text{L}/\text{min}$.

The determination of vessel diameter is critical for calculating the blood flow. To minimize the impact of the low phase difference at the border of the vessel, we select the OCT phase image near a systolic peak to extract the vessel diameter^[29]. A bulk motion algorithm is used to correct the phase background based on a histogram analysis method^[36]. Before starting the detection, the volunteers first adjusted to the darkroom for 10 min to allow the pupils to dilate naturally. The average TRBF of artery is $40.16 \pm 7.48 \mu\text{L}/\text{min}$, and the TRBF of the vein is $43.26 \pm 4.93 \mu\text{L}/\text{min}$ in eight normal eyes.

4. Discussion and Conclusions

In previously published reports by Riva *et al.*^[37], $33 \pm 9.6 \mu\text{L}/\text{min}$ for total arteries and $34 \pm 6.3 \mu\text{L}/\text{min}$ for total vein in 12 eyes were determined by laser Doppler velocimetry (LDV). Using a double-circle scanning pattern, Wang *et al.* measured $45.6 \pm 3.8 \mu\text{L}/\text{min}$ (10 subjects)^[38] and $47.6 \pm 5.4 \mu\text{L}/\text{min}$ (20 subjects)^[39] for the total vein. Haindl *et al.* reported the total venous flow values of $47.1 \pm 5.4 \mu\text{L}/\text{min}$ (20 eyes) utilizing a triple-beam setup. Overall, the values obtained here agree well with previous findings.

Our study has several limitations, including the angular separation between both beams, which cannot be adjusted at will. Secondly, for the poor fixation subjects, our system could not measure their blood flow. To overcome this difficulty, eye-tracking technology is needed. Finally, the vascular outlines are delineated by a human expert, which has certain subjectivity. A more objective boundary delineating software is needed.

In conclusion, we described a beam-displacer-based DDD-OCT system to accurately calculate the blood flow over the cardiac cycle. With two probe beams delay-coded with different optical path lengths, the DDD-OCT system is capable of blood flow imaging in both directions at the same time without crosstalk between two channels, as compared with Refs. [20,21]. The integrated unit of LSLO makes the acquisition process more intuitive and convenient. The *in vivo* study demonstrates the ability of the DDD-OCT to measure the retinal blood flow, which offers promising potential for monitoring retinal blood flow abnormalities in patients.

Acknowledgement

This work was supported by the National Natural Science Foundation of China (Nos. 61975246 and 61505267) and Research Fund for Guangxi Distinguished Experts.

[†]These authors contributed equally to this work.

References

1. T. A. Ciulla, A. Harris, P. Latkany, H. C. Piper, O. Arend, H. Garzozzi, and B. Martin, "Ocular perfusion abnormalities in diabetes," *Acta Ophthalmol.* **80**, 468 (2002).

2. A. Harris, H. S. Chung, T. A. Ciulla, and L. Kagemann, "Progress in measurement of ocular blood flow and relevance to our understanding of glaucoma and age-related macular degeneration," *Prog. Retin. Eye Res.* **18**, 669 (1999).
3. J. C. Hwang, R. Konduru, X. Zhang, O. Tan, B. A. Francis, R. Varma, M. Sehi, D. S. Greenfield, S. R. Sadda, and D. Huang, "Relationship among visual field, blood flow, and neural structure measurements in glaucoma," *Invest. Ophthalmol. Vis. Sci.* **53**, 3020 (2012).
4. D. Huang, E. A. Swanson, C. P. Lin, J. S. Schuman, W. G. Stinson, W. Chang, M. R. Hee, T. Flotte, K. Gregory, C. A. Puliafito, and J. G. Fujimoto, "Optical coherence tomography," *Science* **254**, 1178 (1991).
5. X. Chen, Y. Lei, Y. Wang, and D. Yu, "Resolution enhancement with improved range Doppler algorithm in high numerical aperture OCT," *Chin. Opt. Lett.* **9**, 121001 (2011).
6. D. C. Adler, T. H. Ko, and J. G. Fujimoto, "Speckle reduction in optical coherence tomography images by use of a spatially adaptive wavelet filter," *Opt. Lett.* **29**, 2878 (2004).
7. P. M. Andrews, H. W. Wang, J. Wierwille, W. Gong, J. Verbesey, M. Cooper, and Y. Chen, "Optical coherence tomography of the living human kidney," *J. Innov. Opt. Heal. Sci.* **07**, 1350064 (2014).
8. J. Q. Dong, Q. H. Li, and Y. Q. Hu, "Multi-technique analysis of an ancient stratified glass eye bead by OCT, μ -XRF, and μ -Raman spectroscopy," *Chin. Opt. Lett.* **18**, 090001 (2020).
9. S. Wang, J. Zhou, J. F. Jiang, K. Liu, Q. Han, Y. N. Duan, R. D. Wang, and T. G. Liu, "Multi-channel polarized low-coherence interference synchronous demodulation system based on a matrix charge-coupled device," *Chin. Opt. Lett.* **18**, 071202 (2020).
10. L. Huang, Y. M. Fu, R. X. Chen, S. S. Yang, H. X. Qiu, X. Wu, S. Y. Zhao, Y. Gu, and P. Li, "SNR-adaptive OCT angiography enabled by statistical characterization of intensity and decorrelation with multi-variate time series model," *IEEE Trans. Med. Imaging* **38**, 2695 (2019).
11. H. K. Li, K. Y. Liu, T. T. Cao, L. Yao, Z. Y. Zhang, X. F. Deng, C. X. Du, and P. Li, "High performance OCTA enabled by combining features of shape, intensity, and complex decorrelation," *Opt. Lett.* **46**, 368 (2021).
12. M. Bonesi, A. J. Kennerley, I. Meglinski, and S. Matcher, "Application of Doppler optical coherence tomography in rheological studies: blood flow and vessels mechanical properties evaluation," *J. Innov. Opt. Heal. Sci.* **2**, 431 (2009).
13. O. V. Semyachkina-Glushkovskaya, V. V. Lychagov, O. A. Bibikova, I. A. Semyachkin-Glushkovskiy, S. S. Sindeev, E. M. Zinchenko, M. M. Kassim, A.-F. fatema Ali, A. H. Leith, M. V. Ulanova, and V. V. Tuchin, "The experimental study of stress-related pathological changes in cerebral venous blood flow in newborn rats assessed by doct," *J. Innov. Opt. Heal. Sci.* **6**, 1350023 (2013).
14. G. Liu and Z. Chen, "Advances in Doppler OCT," *Chin. Opt. Lett.* **11**, 011702 (2013).
15. R. Dsouza, H. Subhash, K. Neuhaus, P. M. McNamara, J. Hogan, C. Wilson, and M. J. Leahy, "Feasibility study of phase-sensitive imaging based on multiple reference optical coherence tomography," *Chin. Opt. Lett.* **15**, 090007 (2017).
16. R. A. Leitgeb, R. M. Werkmeister, C. Blatter, and L. Schmetterer, "Doppler optical coherence tomography," *Prog. Retin. Eye Res.* **41**, 26 (2014).
17. D. P. Dave and T. E. Milner, "Doppler-angle measurement in highly scattering media," *Opt. Lett.* **25**, 1523 (2000).
18. G. C. Aschinger, L. Schmetterer, V. Doblhoff-Dier, R. A. Leitgeb, G. Garhöfer, M. Gröschl, and R. M. Werkmeister, "Blood flow velocity vector field reconstruction from dual-beam bidirectional Doppler OCT measurements in retinal veins," *Biomed. Opt. Express* **6**, 1599 (2015).
19. V. Doblhoff-Dier, L. Schmetterer, W. Vilser, G. Garhöfer, M. Gröschl, R. A. Leitgeb, and R. M. Werkmeister, "Measurement of the total retinal blood flow using dual beam Fourier-domain Doppler optical coherence tomography with orthogonal detection planes," *Biomed. Opt. Express* **5**, 630 (2014).
20. C. J. Pedersen, D. Huang, M. A. Shure, and A. M. Rollins, "Measurement of absolute flow velocity vector using dual-angle, delay-encoded Doppler optical coherence tomography," *Opt. Lett.* **32**, 506 (2007).
21. L. M. Peterson, S. Gu, M. W. Jenkins, and A. M. Rollins, "Orientation-independent rapid pulsatile flow measurement using dual-angle Doppler OCT," *Biomed. Opt. Express* **5**, 499 (2014).
22. R. Michaely, A. H. Bachmann, M. L. Villiger, C. Blatter, T. Lasser, and R. A. Leitgeb, "Vectorial reconstruction of retinal blood flow in three

- dimensions measured with high resolution resonant Doppler Fourier domain optical coherence tomography," *J. Biomed. Opt.* **12**, 041213 (2007).
23. S. Makita, T. Fabritius, and Y. Yasuno, "Quantitative retinal-blood flow measurement with three-dimensional vessel geometry determination using ultrahigh-resolution Doppler optical coherence angiography," *Opt. Lett.* **33**, 836 (2008).
 24. B. Baumann, B. Potsaid, M. F. Kraus, J. J. Liu, D. Huang, J. Hornegger, A. E. Cable, J. S. Duker, and J. G. Fujimoto, "Total retinal blood flow measurement with ultrahigh speed swept source/Fourier domain OCT," *Biomed. Opt. Express* **2**, 1539 (2011).
 25. W. Choi, B. Baumann, J. J. Liu, A. C. Clermont, E. P. Feener, J. S. Duker, and J. G. Fujimoto, "Measurement of pulsatile total blood flow in the human and rat retina with ultrahigh speed spectral/Fourier domain OCT," *Biomed. Opt. Express* **3**, 1047 (2012).
 26. Y. Wang, B. A. Bower, J. A. Izatt, O. Tan, and D. Huang, "In vivo retinal blood flow measurement by Fourier domain Doppler optical coherence tomography," *J. Biomed. Opt.* **12**, 041215 (2007).
 27. Y. Wang, B. A. Bower, J. A. Izatt, O. Tan, and D. Huang, "Retinal blood flow measurement by circumpapillary Fourier domain Doppler optical coherence tomography," *J. Biomed. Opt.* **13**, 064003 (2008).
 28. W. Trasischker, R. M. Werkmeister, S. Zotter, B. Baumann, T. Torzicky, M. Pircher, and C. K. Hitzenberger, "In vitro and in vivo three-dimensional velocity vector measurement by three-beam spectral-domain Doppler optical coherence tomography," *J. Biomed. Opt.* **18**, 116010 (2013).
 29. R. Haindl, W. Trasischker, A. Wartak, B. Baumann, M. Pircher, and C. K. Hitzenberger, "Total retinal blood flow measurement by three beam Doppler optical coherence tomography," *Biomed. Opt. Express* **7**, 287 (2016).
 30. A. Wartak, R. Haindl, W. Trasischker, B. Baumann, M. Pircher, and C. K. Hitzenberger, "Active-passive path-length encoded (APPLE) Doppler OCT," *Biomed. Opt. Express* **7**, 5233 (2016).
 31. A. Wartak, F. Beer, B. Baumann, M. Pircher, and C. K. Hitzenberger, "Adaptable switching schemes for time-encoded multichannel optical coherence tomography," *J. Biomed. Opt.* **23**, 056010 (2018).
 32. C. Blatter, S. Coquoz, B. Grajciar, A. S. G. Singh, M. Bonesi, R. M. Werkmeister, L. Schmetterer, and R. A. Leitgeb, "Dove prism based rotating dual beam bidirectional Doppler OCT," *Biomed. Opt. Express* **4**, 1188 (2013).
 33. R. M. Werkmeister, N. Dragostinoff, M. Pircher, E. Götzinger, C. K. Hitzenberger, R. A. Leitgeb, and L. Schmetterer, "Bidirectional Doppler Fourier-domain optical coherence tomography for measurement of absolute flow velocities in human retinal vessels," *Opt. Lett.* **33**, 2967 (2008).
 34. S. Norrby, P. Piers, C. Campbell, and M. V. D. Mooren, "Model eyes for evaluation of intraocular lenses," *Appl. Opt.* **46**, 6595 (2007).
 35. C. Blatter, B. Grajciar, L. Schmetterer, and R. A. Leitgeb, "Angle independent flow assessment with bidirectional Doppler optical coherence tomography," *Opt. Lett.* **38**, 4433 (2013).
 36. C. Kolbitsch, T. Schmoll, and R. A. Leitgeb, "Histogram-based filtering for quantitative 3D retinal angiography," *J. Biophotonics* **2**, 416 (2009).
 37. C. E. Riva, J. E. Grunwald, S. H. Sinclair, and B. L. Petrig, "Blood velocity and volumetric flow rate in human retinal vessels," *Invest. Ophthalmol. Vis. Sci.* **26**, 1124 (1985).
 38. Y. Wang, A. Lu, J. Gil-Flamer, O. Tan, J. A. Izatt, and D. Huang, "Measurement of total blood flow in the normal human retina using Doppler Fourier-domain optical coherence tomography," *Br. J. Ophthalmol.* **93**, 634 (2009).
 39. Y. Wang, A. A. Fawzi, R. Varma, A. A. Sadun, X. Zhang, O. Tan, J. A. Izatt, and D. Huang, "Pilot study of optical coherence tomography measurement of retinal blood flow in retinal and optic nerve diseases," *Invest. Ophthalmol. Vis. Sci.* **52**, 840 (2011).